metals

MDPI

Article

Cobalt and Manganese Extraction from Ocean Nodules by Co-Processing with Steel Metallurgical Slag

Kevin Pérez [1], Norman Toro [2], Pedro Robles [3], Sandra Gallegos [2], Edelmira Gálvez [4], Francisco Javier González [5], Egidio Marino [5] and Pía C. Hernández [1,6,*]

1 Departamento de Ingeniería Química y Procesos de Minerales, Facultad de Ingeniería, Universidad de Antofagasta, Av. Angamos 601, Antofagasta 1240000, Chile; kevin.perez.salinas@ua.cl
2 Faculty of Engineering and Architecture, Universidad Arturo Prat, Iquique 1100000, Chile; notoro@unap.cl (N.T.); sandra@kidcoedu.org (S.G.)
3 Escuela de Ingeniería Química, Pontificia Universidad Católica de Valparaíso, Valparaíso 2340000, Chile; pedro.robles@pucv.cl
4 Departamento de Ingeniería Metalúrgica y Minas, Universidad Católica del Norte, Antofagasta 1270709, Chile; egalvez@ucn.cl
5 Instituto Geológico y Minero de España (IGME-CSIC), Ríos Rosas, 23, 28003 Madrid, Spain; fj.gonzalez@igme.es (F.J.G.); e.marino@igme.es (E.M.)
6 Centro de Economía Circular en Procesos Industriales (CECPI), Facultad de Ingeniería, Universidad de Antofagasta, Av. Angamos 601, Antofagasta 1270300, Chile
* Correspondence: pia.hernandez@uantof.cl; Tel.: +56-55-2-637525

Abstract: Polymetallic nodules, also called manganese nodules (due to their high content of this element), contain various valuable metals such as Cu, Ni and Co. These seabed minerals are a good alternative source of Co and Mn due to the decrease in the grade of mineral deposits on the earth's surface. For the treatment of manganese nodules, acid-reducing leaching is apparently the most attractive, due to its low cost compared to other processes, short operational times, and it is more friendly to the environment. In this investigation, the extraction of Mn and Co from manganese nodules from two different locations was studied in acid media and by reusing a steel slag obtained from a steel smelting process. An ANOVA analysis was performed to determine the most appropriate Manganese Nodule/$Fe_{(res)}$ ratio and time to dissolve Co and Mn from the nodules. Effect of temperature on the process was evaluated, and then a residue analysis was carried out. Finally, it was discovered that the best results were obtained when working at 60 °C in a time of 15 min, obtaining extractions of approximately 98% Mn and 55% Co. Additionally, the formation of polluting elements was not observed, nor the precipitation of Mn and Co species in the studied residues.

Keywords: marine nodules; cobalt; manganese; leaching; iron slag

Citation: Pérez, K.; Toro, N.; Robles, P.; Gallegos, S.; Gálvez, E.; González, F.J.; Marino, E.; Hernández, P.C. Cobalt and Manganese Extraction from Ocean Nodules by Co-Processing with Steel Metallurgical Slag. *Metals* **2023**, *13*, 1079. https://doi.org/10.3390/met13061079

Academic Editors: Srecko Stopic and Daniel Assumpcao Bertuol

Received: 11 April 2023
Revised: 25 May 2023
Accepted: 1 June 2023
Published: 7 June 2023

1. Introduction

In 1868, minerals composed of chemical sediments formed from concentric layers of Fe and Mn oxyhydroxides around a nucleus, called polymetallic nodules, were discovered in the bottom of the Kara Sea (Arctic Ocean) [1,2]. Then, in the Challenger expedition (1873–1876), it was discovered that these mineral resources were present in most of the world's oceans [3,4]. Polymetallic nodules, also called manganese nodules (due to their high content of this element), contain various valuable metals such as Cu, Ni and Co, as well as traces of Mo, Ti, Pb, Li, Pt, Ti, Zr and Zn and light and heavy rare earth elements [5], which is why they are considered the most valuable oceanic mineral resource [6–8]. Marine manganese nodules are commonly formed by the combination of two processes: hydrogenetic, when all constituents are derived from cold seawater; and diagenetic, when all constituents are derived from cold sediment pore water [9]. The size of the nodules usually between millimeters and several centimeters.

Among the various elements previously mentioned in manganese nodules, the two most abundant are manganese and cobalt. Manganese is the 12th most abundant element on the planet, covering about 0.1% of the Earth's crust [10]. However, despite this abundance on the planet's surface, manganese minerals are widely disseminated, currently making it difficult to find high-grade deposits [11]. On the other hand, cobalt is a scarce element on the planet, representing 0.003% of the Earth's crust. Furthermore, most of the world's cobalt supply is controlled by the Democratic Republic of the Congo (60% of production), while no other country supplies more than 6% [12].

In addition, it is important to mention the decrease in the grades of mineral deposits on the Earth's surface over the years, and the current need to obtain a greater amount of "critical" metals necessary for the development and manufacture of environmentally friendly technologies [5,13,14]. For example, in 1942 in Chile, the average cobalt grade was approximately 5%, while currently the country's average cobalt grade is less than 1%, reaching a maximum of 1.6% in some specific areas [15]. This situation forces large mining companies to increase their production to compensate for the drop in mineral grades, but in turn, this produces a greater increase in environmental liabilities, such as tailings generated from flotation processes (for example, in large-scale copper mining, 150 tons of tailings are generated for every ton of copper) [11]. This forces the search for new alternative sources to obtain metals, with underwater mining being a good option to obtain these resources, since it is estimated that the largest reserves of cobalt and manganese in the world are found in the seabed [15,16].

For the extraction of metals from manganese nodules, various pyro-metallurgical processes have been proposed, such as segregation by roasting [17] and reduction by smelting [18,19]; pyro-hydrometallurgical processes, such as segregation by roasting in the presence of chloride agents [20], extraction by sulphation roasting and subsequent leaching [21,22], reduction by roasting and subsequent selective ammonia leaching [23]; pyrolysis and subsequent leaching with sulfuric acid [24]; and hydrometallurgical processes, such as high temperature and pressure leaching (autoclave) [25,26], leaching with the use of reducing agents [27–29], bioleaching [30,31] and galvanic leaching [32].

Among the various technologies previously explained for the extraction of metals from marine nodules, acid-reducing leaching is apparently the most attractive, due to its low cost compared to the other technologies, short operational times and improved environmental friendliness. Among the various possible reducing agents (SO_2 [33], Fe [34], $(NH_4)_2SO_4$ [35], paper [36], NH_3–$(NH_4)_2CO_3$ medium [37], etc.), iron is a very good alternative because it is abundant, inexpensive and can be obtained from industrial waste [34]. In recent years, various works have been carried out to obtain manganese from polymetallic nodules with the use of iron-reducing agents. In the research carried out by Torres et al. [38], the use of different iron-reducing agents used in previous studies by other researchers was compared, such as: pyrite, ferrous ions, sponge iron and tailings. In the study by Torres et al. [38], agents were worked in stirred reactors, at a low particle size of the manganese nodules ($-140 + 100$ µm) and reducing agents ($-75 + 53$ µm), with the use of sulfuric acid at different concentrations (0.1, 0.5 and 1 mol/L), different ratios of reducing agent/marine nodule (3/1, 2/1, 1/1 and 1/2), all at room temperature (except in the case of pyrite, which was worked at 60 °C, since this mineral is more refractory and it was necessary to raise the temperature for it to react and form $Fe_2(SO_4)_3$). In their results, the researchers observed that in ferrous ions, sponge iron and tailings, at a ratio of reducing agent/marine nodule of 3/1 and 2/1, the redox potential values remained low (in a range between 0.5 and −0.4 V), allowing work at a low concentration of sulfuric acid (0.1 mol/L) and to obtain manganese extractions over 60% in a time period of 15 min, while for the use of pyrite as a reducing agent, it was necessary to work at FeS_2/marine nodule ratios of 3/1 and sulfuric acid concentrations of 1 mol/L to achieve an extraction of 30% manganese in 30 min.

For the extraction of manganese and cobalt from polymetallic nodules in an acid medium, at room temperature and with iron as a reducing agent, previous research has shown that it is possible to recover both elements [15,34]. Manganese commonly occurs in

three oxidation states (II, III and IV), where the comparative stability of each oxidation state in solution is greatly affected by Eh and pH [39]. By working in an acid-reducing leaching, it is possible to efficiently convert the Mn(IV) of the manganese ore into Mn(II), while to recover cobalt, as can be seen in Figure 1, it is possible to recover it as Co(II) in potential ranges between 0.8 and −0.25 V, a redox potential range that is within the range for the recovery of Mn(II) (1.4 and −1.2 V).

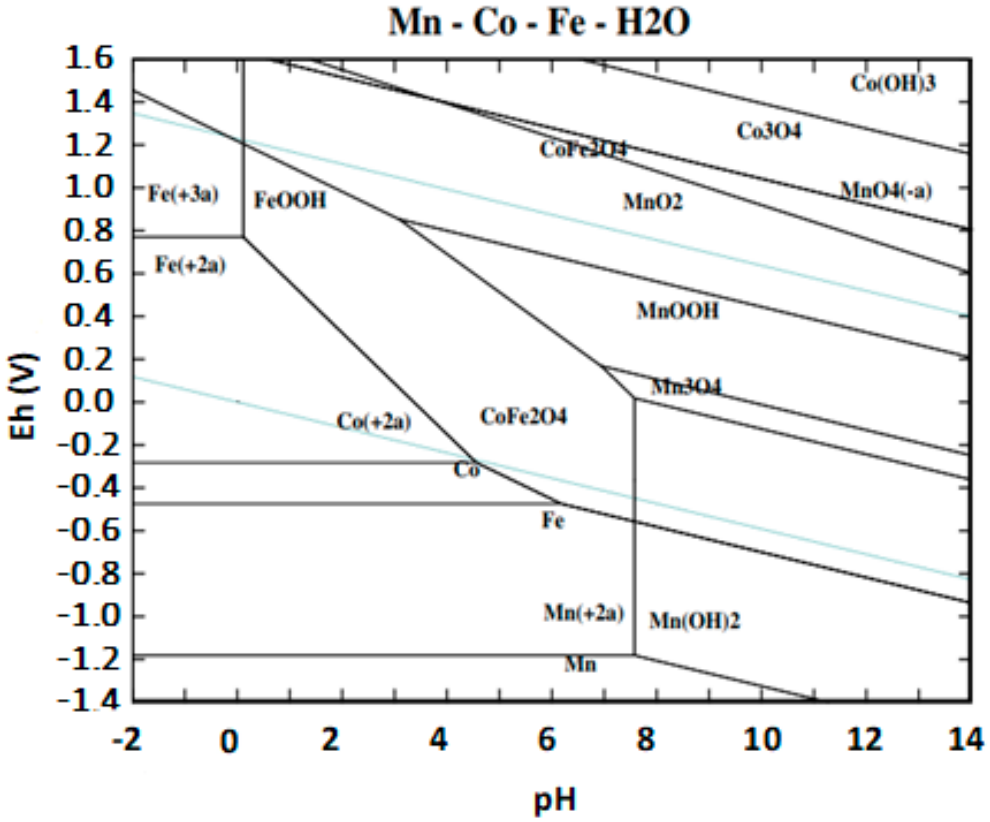

Figure 1. Potential pH diagram for the Mn-Co-Fe-H_2O system at 25 °C and unit activity [40].

Among the various iron residues that are produced by the industry, one never mentioned is the "slag" product from a steel foundry, composed mainly of magnetite and whose main characteristic is its form of disintegrated flakes of different sizes. This product is difficult to compact, with a tendency towards volatility of solids; therefore, it cannot be reused in direct casting processes. In addition, it has size differences in its conformation (ranges from 1 to 10 mm on average), which generates an additional difficulty in the direct compaction process, producing interstitial spaces with a lack of cohesion of the particles; therefore, it is necessary to add to the product agents that allow the material to bind. Some companies in the steel industry in Chile have tried to include chemical additives that make it possible to bind and help improve the cohesion of the material particles, through an easy process and at a limited cost, which allows an industrial process to be carried out, and to be used commercially in terms of this waste product. However, they have not been successful so far in this search.

The objective of this research is to reuse these industrial residues from steel companies in Chile in order to process manganese nodules in an acid medium. For this, a novel process is proposed with the use of this additive and sulfuric acid at room temperature to recover Mn and Co. In Table 1, the Gibbs free energy values are presented, calculated from the standard reduction potential values where it can be seen that the proposed reactions are thermodynamically favorable.

Table 1. Reactions proposed for the dissolution of Mn and Co from marine nodules with H_2SO_4 at room temperature (based on HSC Chemistry 6).

Reaction	ΔG° (kJ)	Equation
Fe_3O_4 (s) + $4H_2SO_4$ (l) = $FeSO_4$ (aq) + $Fe_2(SO_4)_3$ (s) + $4H_2O$ (l)	−264.27	(1)
$2FeSO_4$ (aq) + $2H_2SO_4$ (aq) + MnO_2 (s) = $Fe_2(SO_4)_3$ (s) + $2H_2O$ (l) + $MnSO_4$ (aq)	−221.44	(2)
CoO + H_2SO_4 = $CoSO_4$ + H_2O	−115.43	(3)
Co_3O_4 + $4H_2SO_4$ + $2FeSO_4$ = $3CoSO_4$ + $4H_2O$ + $Fe_2(SO_4)_3$	−354.18	(4)

It is important to note that Chile is a country that produces sulfuric acid. It has potential extensive areas covered by manganese nodules within its Exclusive Economic Zone and also must seek a use for the waste generated in the different local metal industries; therefore, this manuscript proposes a low-cost and more environmentally friendly alternative to other methods (flotation and/or smelting) to obtain aqueous solutions of cobalt and manganese.

2. Materials and Methods

2.1. Polymetallic Nodules

Sample 1 of marine nodules was collected in the 1970s from the Blake Plateau in the NW Atlantic Ocean. This was ground in a porcelain mortar to sizes ranging from −140 to +100 μm. The ground sample was analyzed with atomic emission spectrometry via induction-coupled plasma (ICP-AES) in the applied geochemistry laboratory of the Department of Geological Sciences of the Universidad Católica del Norte. Sample 2 was a Fe-rich nodule collected using benthic dredge from the northeast middle slope of the Gulf of Cadiz (NE Atlantic Ocean). Bulk mineralogical X-ray diffraction (XRD) profile from 2θ = 2–60° in 0.005 steps was obtained in the nodule using XPERT PRO of PANalytical, Cu-Kα radiation (35 Kv, 40 mA) with a graphite monochromater, High Score software and the ICDD database. Bulk chemical composition was measured for major (Al, Fe, Mn, Ca, Mg, Si, K, Ti and P) and trace elements (Co, Cu and Ni) by X-ray fluorescence (XRF) using a MagiX of PANalytical instrument with Rh radiation. Na was measured using atomic absorption with a VARIAN FS-220. The accuracy of the data was checked by using international standard reference materials, and precisions based on duplicate samples were found to be better than ±5%. The results of the elemental characterization of the manganese nodules are presented in Tables 2 and 3.

Table 2. Chemical analysis of the manganese nodules.

	Components (wt. %)		
	Mn	**Fe**	**Co**
Sample 1 (Blake Plateau)	15.96	0.45	0.29
Sample 2 (Gulf of Cadiz)	7.05	35.45	0.0073

Table 3. Major chemical components of manganese nodules.

	Components (wt. %)								
	MgO	**Al_2O_3**	**SiO_2**	**P_2O_5**	**K_2O**	**CaO**	**TiO_2**	**MnO_2**	**Fe_2O_3**
Sample 1 (Blake Plateau)	3.54	3.69	2.97	7.20	0.33	22.48	1.07	29.85	26.02
Sample 2 (Gulf of Cadiz)	3.39	3.47	10.6	0.45	0.63	2.77	0.22	9.11	50.7

Sample 1 is a regular-shaped ferromanganese nodule (Figure 2A). Sample 1 was analyzed with Bruker® M4-Tornado μ-XRF desktop equipment. The sample can be divided into two principal components based on color: (i) the black-brown mineral phases (the dominant phase) (Figure 2B), and (ii) the white-cream mineral phases (as veins). The

black mineral phase is dominantly a Mn/Fe-Oxide/Hydroxide mineral(s) of varying ratios. Although this phase is apparently homogeneous in an optical image, μ-XRF elemental maps allow observation of two different areas with distinctive distributions of minor elements (Figure 2C). The nodule is comprised of a P-Co-Pb trace content pre-existent Fe-Mn nodule fragment, forming the core, with concentric Cr-Ni-As trace content Mn-Fe layers precipitated around it at later stages. An even later event caused Sr-Cu-Zn calcic fluids to penetrate the nodule, crystallizing the white-cream mineral phases along the contact between core and outside layers, as well as radial veins in the outer portion of the nodule. The cream mineral in the veins is possibly a carbonate with Sr-associated enrichment (Figure 2D). Sample 1 mainly contains calcite, magnesium, manganese and iron (Figure 3). The mineralogy of the nodule is dominated by goethite and lepidocrocite with minor content of 7 Å manganates, 10 Å manganates, pyrolusite, quartz and phyllosilicates (illite, smectite, kaolinite).

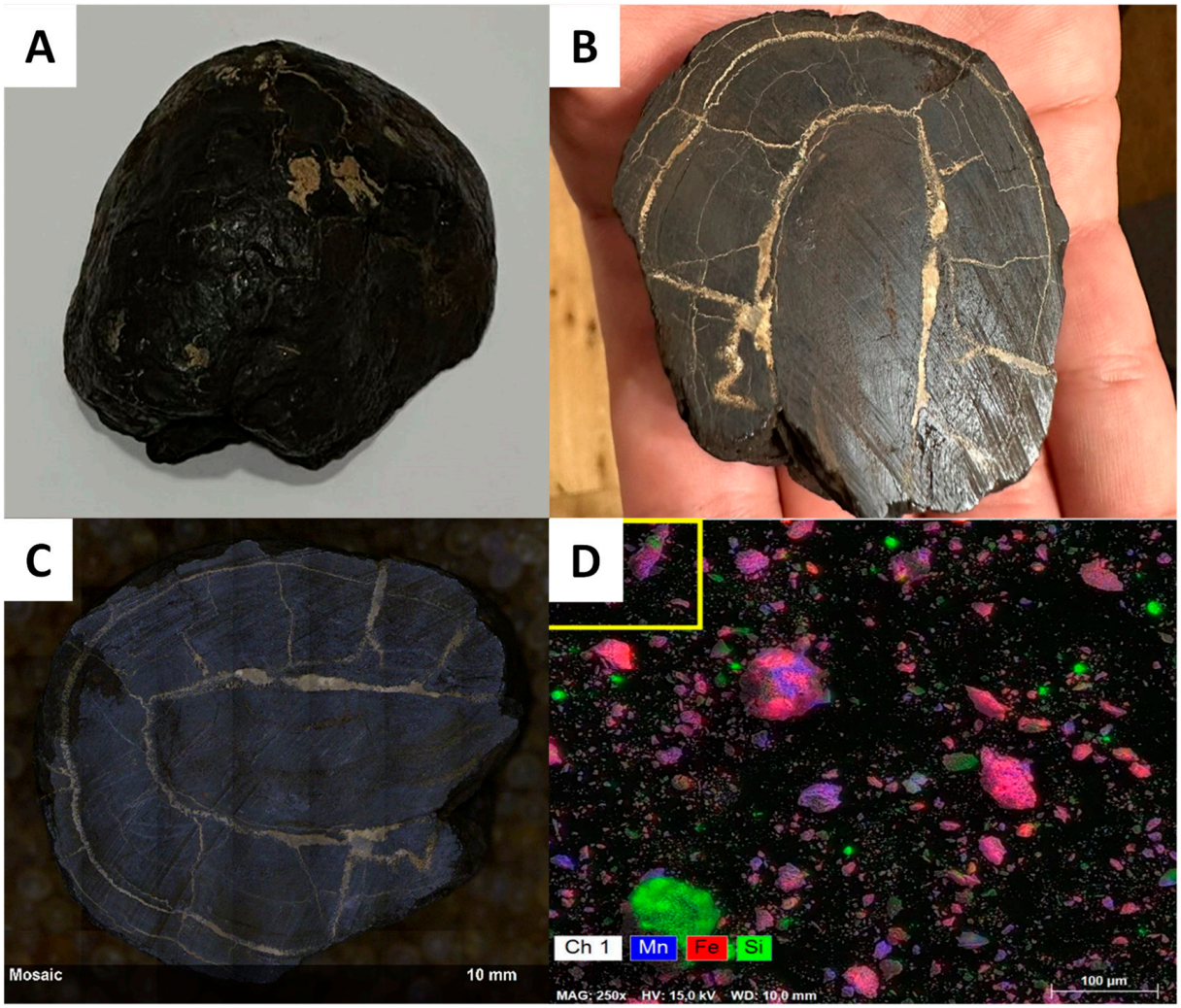

Figure 2. (**A**) Ferromanganese nodule recovered in Blake Plateau. (**B**) Section and internal structure of the nodule. (**C**) Bruker M4 Tornado optical image. (**D**) SEM photomicrograph with EDS analysis.

Sample 2 is a tabular-to-irregular-shaped ferromanganese nodule (Figure 4A). The external color of the nodule ranges from predominantly yellow-orange to black. Internally, the nucleus is not distinguished from the layers that show massive, laminated mottled-to-dendritic textures (Figure 4B,C). The layers show a dominant orange color (in which Fe oxy-hydroxides predominate) and minor black (in which Mn oxides predominate) in the edge part of the nodule. Under the petrographic and electronic microscopes, the layers

are usually formed by a micro-sparitic mosaic of subidiomorphic to idiomorphic zoned crystals (2–10 μm) of Fe–Mn oxy-hydroxides and dispersal carbonate bioclasts and silicates (Figure 4D).

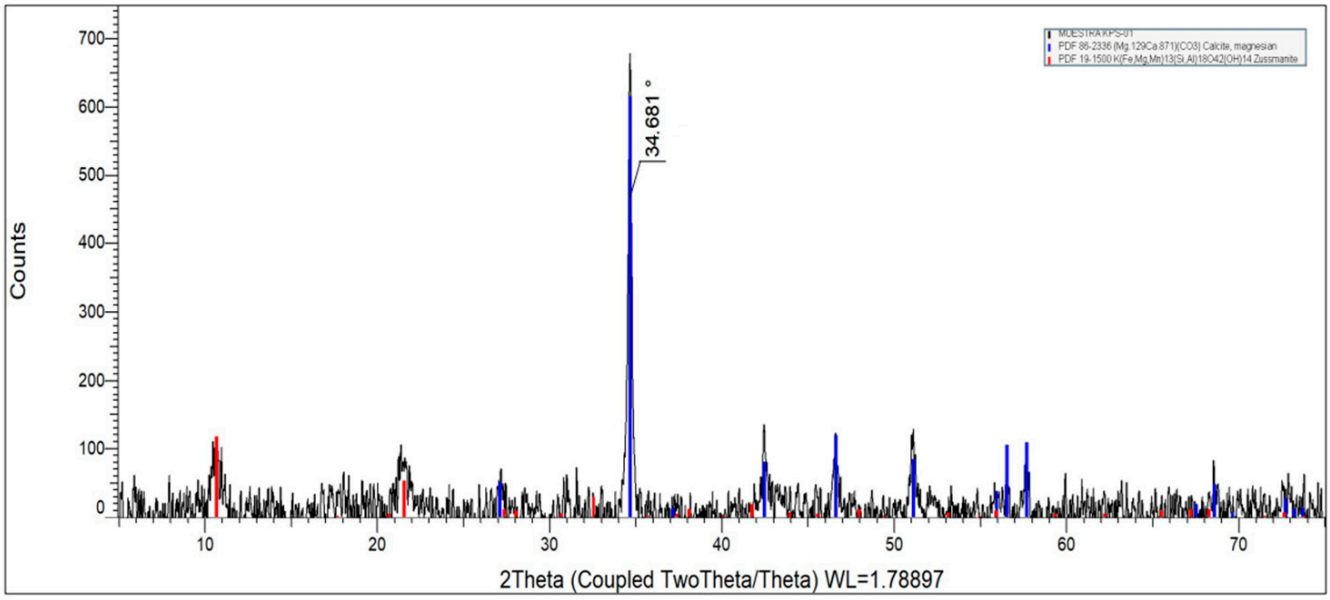

Figure 3. XRD pattern of sample 1 (bulk sample).

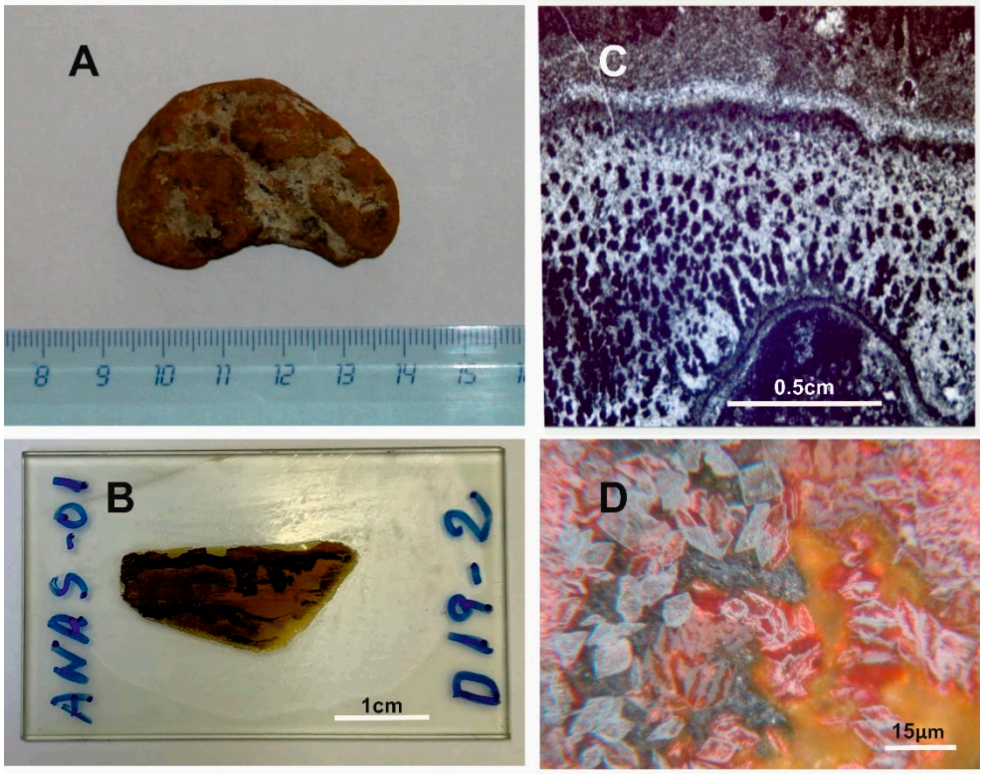

Figure 4. (**A**) Ferromanganese nodule ANAS01/D19-02 recovered in the Gulf of Cadiz. (**B**) Section and internal structure of the nodule. (**C**,**D**) Microscopic internal features. (**C**) Mottled-to-dendritic textures. (**D**) Oxide layer showing rhomboidal crystal sections of goethite–birnessite surrounded by Mn oxides and silicates. Sample 2 contains minor quantities of Ni (116 μg/g) and Cu (43 μg/g) in bulk analysis.

The XRD analyses (Figure 5) show the abundance of goethite with the d (110) ranging between 4.161 and 4.189 Å, and Mn-oxyhydroxides (pyrolusite, 7 Å-manganates and 10 Å-manganates) in lesser abundance. The silicates that are more abundant are quartz, smectite and illite.

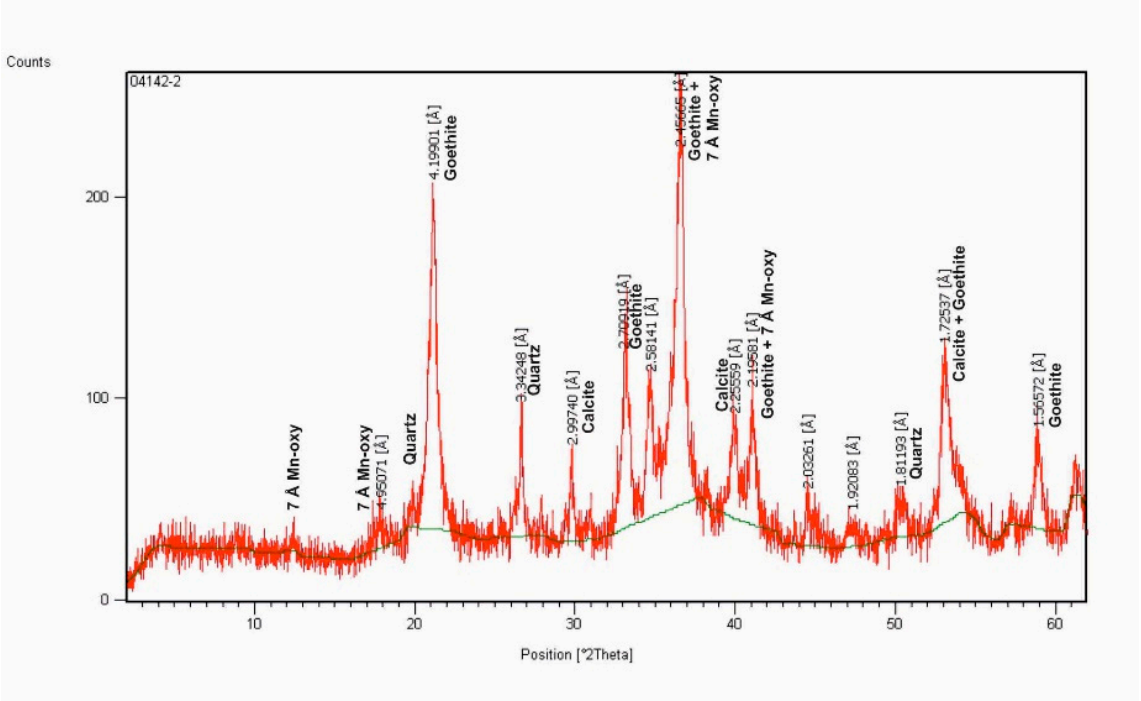

Figure 5. XRD pattern of sample 2 (bulk sample).

2.2. Iron Residue ($Fe_{(res)}$)

The steel residue used is a "slag" obtained from a steel smelting process of the CAP Company in Antofagasta, Chile. This residue has a content of 99.73% Fe_3O_4 and 0.27% metallic iron. Its initial size is between 1 to 10 mm, but it was reduced in size in a mortar until it reached a size between −140 to +100 µm.

2.3. Leaching Tests

The leaching tests were carried out in a 200 mL glass reactor at 0.1 solid-to-liquid ratio (100 mL of acid solution). A total of 10 g of the mineral (manganese nodules) was kept under agitation and suspension using a 5-position magnetic stirrer (IKA ROS, CEP 13087-534, Campinas, Brazil) at 600 rpm and a particle size of −140 to + 100µm. The temperature was controlled using an oil-heated circulator (Julabo, St. Louis, MO, USA). The temperature range tested in the experiments was 25 to 60 °C. All tests were performed in duplicate, and analyses were carried out using 5 mL undiluted samples and AAS with a ≤5% variation quotient and 5–10% relative difference. The pH and oxidation-reduction potential were measurements of the leaching solutions and were carried out in a pH-ORP meter (HANNA HI-4222, St. Louis, MO, USA). The ORP solution was measured using an ORP electrode cell composed of a platinum-employed electrode and a saturated Ag/AgCl reference electrode.

2.4. Experimental Design

The effect of the independent variables on the extraction of Mn was studied using the surface optimization methodology [41]. The Central Composite Face (CCF) design and a quadratic model were applied to the experimental design for the extraction of Mn.

The Response Surface Methodology (RSM) is a set of statistical techniques used to model and analyze problems in which a response variable is influenced by other explana-

tory or independent variables. The initial purpose of these techniques is to design an experiment that provides reasonable values of the response variable and to determine the mathematical model that best fits the data obtained (goodness-of-fit statistics such as MAD, MSE, MAPE and R^2 are used for this purpose), among others [42]. The ultimate goal is to establish the values of the factors that optimize the value of the response variable. This is achieved by determining the optimal operating conditions of the system [43].

The difference between (RSM) and a current experimental design (DOE) is that an experimental design aims to identify the winning combination or sample among all those that have been tested. Instead, RSM aims to locate the optimal operating conditions of the process for the range of sampled parameters or domain of the independent variables [44].

The methodology used consisted of manganese nodule leaching experiments, carrying out 9 experimental tests, studying the effects of the Mn nodule/$Fe_{(res)}$ rate and time on each of the dependent variables and Mn and Co recovery (see Table 4). For the modeling and experimental design, Minitab 18 software was used [45], allowing us to investigate the linear effects, the interactions and the quadratic effects of the independent variables in the responses. The experimental data were adjusted by means of a multiple regression analysis to a quadratic model, considering only those factors that helped explain the variability of the model and that had a high statistical significance.

Table 4. Experimental parameters for central composite face design.

Parameter	Bass	Medium	Tall
Time (min)	10	20	30
Mn nodule/$Fe_{(res)}$	2/1	1/1	1/2
Coding	−1	0	1

The general form of the experimental model is given by:

$$Y = (overall\ constant) + (linear\ effects) + (interaction\ effects) + (curvature\ effects) \quad (5)$$

$$Y = b_0 + \sum_{i=1}^{n} b_i x_i + \sum_{i=1}^{n} \sum_{j=1}^{n} b_{ij} x_i x_j \quad (6)$$

where x_i represents the variables of time and Mn nodule/$Fe_{(res)}$ ratio, while the parameters b are the coefficients of the independent variables. The ranges of values of the aforementioned parameters that were used for the design of the experimental model are presented in Table 5. For manganese and cobalt recovery calculations, initial concentrations of 15,960 and 7050 ppm were considered, respectively, and the recovery was the quotient between the concentration of each test and the initial.

Table 5. Experimental design and experimental data for Mn and Co extraction.

Test	Time (min)	Manganese Nodule/$Fe_{(res)}$	Mn Concentration (ppm)	Co Concentration (ppm)	Mn Recovery (%)	Co Recovery (%)
1	10	2/1	7182.00	874.20	45.00	12.40
2	10	1/1	9615.90	1505.18	60.25	21.35
3	10	1/2	11,810.40	2291.25	74.00	32.50
4	20	2/1	6336.12	1593.30	39.70	22.60
5	20	1/1	11,251.80	1910.55	70.50	27.10
6	20	1/2	12,408.90	2379.38	77.75	33.75
7	30	2/1	7102.20	1737.83	44.50	24.65
8	30	1/1	12,448.80	2217.23	78.00	31.45
9	30	1/2	13,127.10	2650.80	82.25	37.60

The values of the variables are encoded in the model. The following equation is used to transform a real value Z_i to a coded value X_i that conforms to the experimental design [46].

$$X_i = \frac{Z_i - \frac{Z_{high}+Z_{low}}{2}}{\frac{Z_{high}-Z_{low}}{2}} \quad (7)$$

where Z_{high} and Z_{low} are the highest and lowest values of the variable i, respectively. The R^2 statistics and p values indicate whether the model obtained is adequate to describe the mineral extraction under the set of sampled values. The R^2 coefficient measures the proportion of total variability of the dependent variable with respect to its mean that is explained by the regression model, while the p-values represent statistical significance, indicating whether there is a statistically significant association between the response variable and the independent variable [47].

2.5. Temperature Effect

Previous studies have shown the positive effect of temperature on the dissolution of elements from marine nodules. Saldana et al. [48] indicated that when working at temperatures above 80 °C, there is a rapid dissolution of Mn, and under this condition other operational variables such as particle size, agitation speed, acid concentration and reducing agent become irrelevant, being only necessary a low concentration of the latter in the system. On the other hand, for room temperature and moderate temperatures, it has been shown that working at high concentrations of reducing agent increases the dissolution of Mn and Co [3,34,49].

For the reasons stated, the experimental tests were carried out with the following operational parameters: Mn nodules/$Fe_{(res)}$ ratio of 1/2, 600 rpm, −140 to +100 µm and H_2SO_4 concentration of 0.1 mol/L.

3. Results and Discussion

3.1. Effect of Variables

The analysis of the contour plots (see Figures 6 and 7) indicates that both the time and the Mn nodules/$Fe_{(res)}$ rate have a directly proportional relationship with the response variables Mn and Co recovery, while the main effects analysis (see Figure 8) indicates that the explanatory factor that has a greater effect on both explained variables is the Mn nodules/$Fe_{(res)}$ ratio.

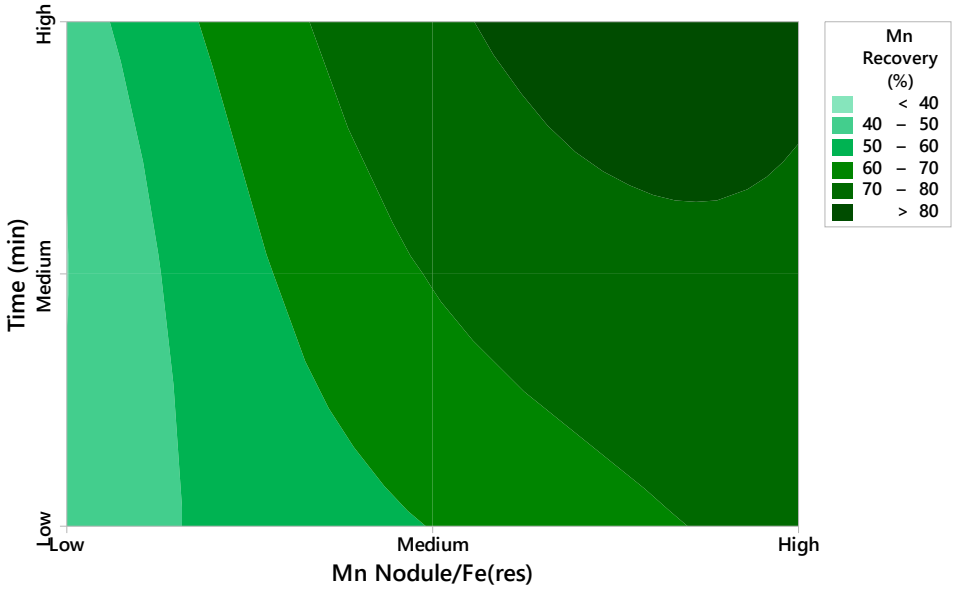

Figure 6. Contour plot of Mn recovery (%) vs. time (min); Mn nodule/$Fe_{(res)}$.

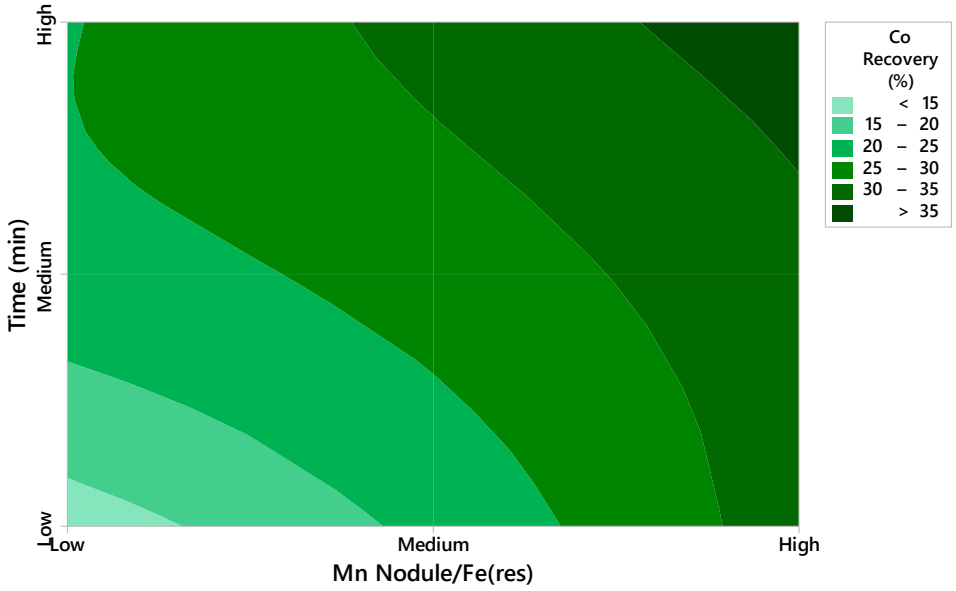

Figure 7. Contour plot of Co recovery (%) vs. time(min); Mn nodule/$Fe_{(res)}$.

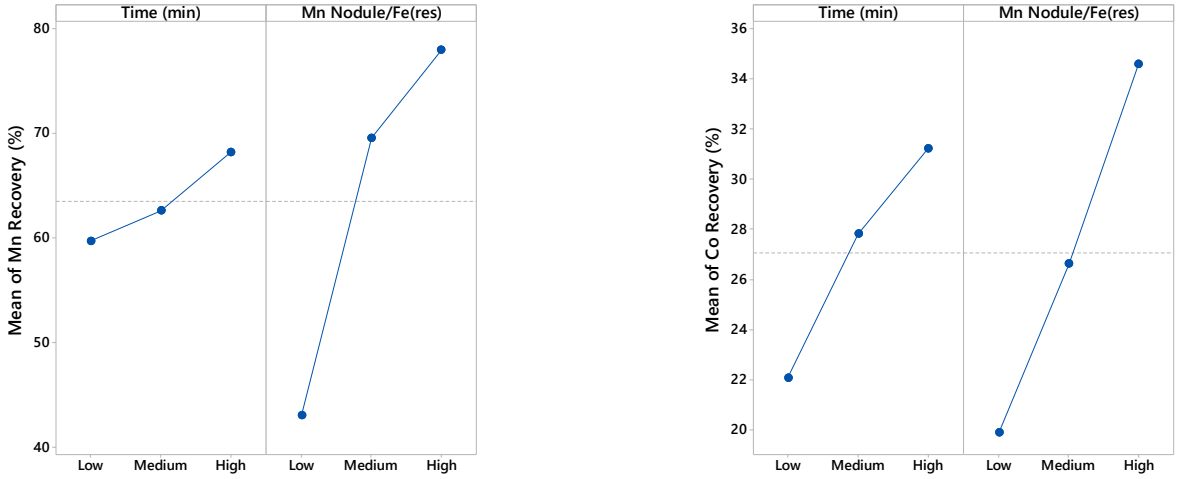

(**a**) (**b**)

Figure 8. Plot of main effects of Mn recovery (**a**) and Co recovery (**b**).

Based on the information obtained from the ANOVA analysis, and after removing non-significant coefficients from the multiple regression models, the analytical models fitted to predict mineral extraction over the range of sampled experimental conditions are presented in Equations (8) and (9), where there is no significant effect of the interactions and the curvature terms ($p > 0.05$) on the recovery of Mn and Co, with only the linear effects of time and ratio Mn nodule/$Fe_{(res)}$ being significant.

$$\text{Mn Recovery (\%)} = 69.58 + 4.25\ \text{Time (min)} + 17.47\ \text{Mn nodule/Fe}_{(res)} - 9.05\ [\text{Mn nodule/Fe}_{(res)}]^2 \quad (8)$$

$$\text{Co Recovery (\%)} = 27.044 + 4.575\ \text{Time (min)} + 7.367\ \text{Mn nodule/Fe}_{(res)} - 1.788\ \text{Time (min)} * \text{Mn nodule/Fe}_{(res)} \quad (9)$$

The ANOVA test of both models indicates that the presented multiple linear regression models are adequate to represent the extraction of Mn and Co under the range of the sampled parameters, while the statistics of the Mn and Co recovery models are presented in Table 6.

Table 6. Goodness-of-fit statistics of the multiple linear regression models.

Model	F-Value	*p*-Value	R^2	R^2–adj	R^2–pred
Mn Recovery	34.47	0.001	95.39	92.62	82.52
Co Recovery	55.39	0.000	97.08	95.33	87.59

There is no lack of fit of the models, and the values of R^2 (95.39% and 97.08%, for the recoveries of Mn and Co, respectively) validate it. ANOVA analysis shows that the indicated factors have an effect on the manganese extraction of $F_{regression} > F_{Table,\ 95\%\ confidence\ level}$ F (5.4095). Additionally, the *p* values of both the models and each individual parameter represented in Equations (9) and (10) indicate that the models are statistically significant, and the goodness-of-fit indicators, together with the normal distribution of the residuals, indicate that the models present a good fit to the experimental data (see Figure 9).

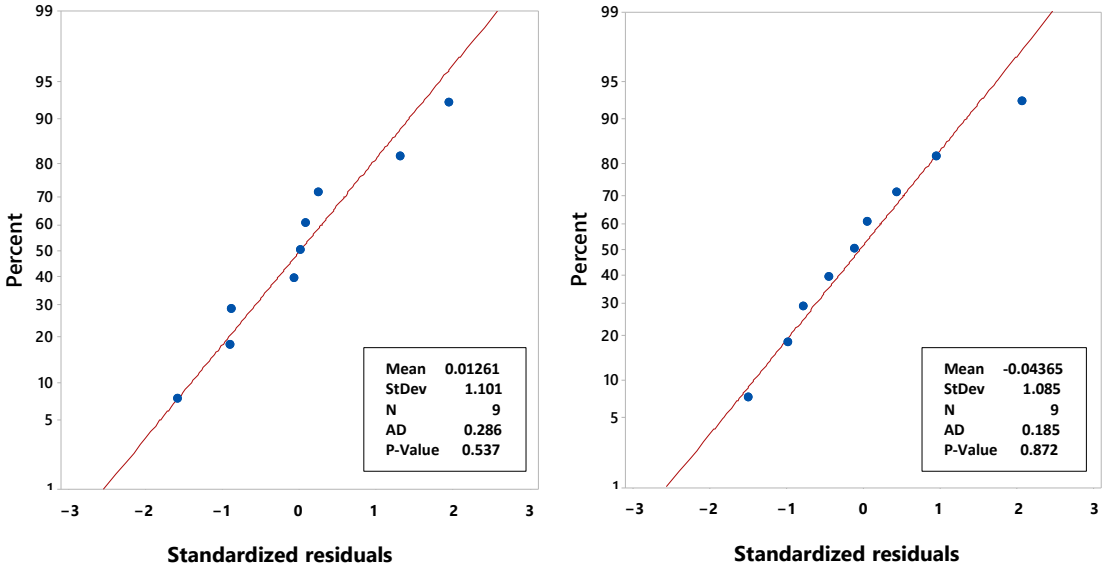

Figure 9. Probability plot of the standardized residues for the recovery of Mn (**a**) and Co (**b**).

In the response surface graph presented in Figure 10, it can be seen that the recovery of Mn and Co increases both with time and at high rates of the Mn nodule/$Fe_{(res)}$ ratio, presenting a greater marginal variation to the ratio factor than at the time.

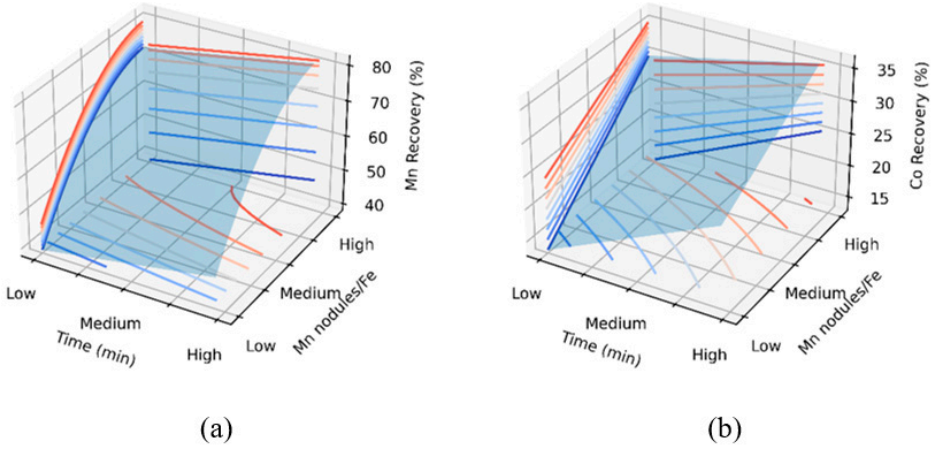

Figure 10. Response surface of the independent variables time (min) and Mn nodule/$Fe_{(res)}$ ratio in the dependent variables Mn and Co recovery (%) ((**a**): Mn recovery, (**b**): Co recovery).

3.2. Temperature in Leaching Tests

Figure 11 shows the effect of temperature on the dissolution of Mn and Co from marine nodules. It is possible to see that working at high temperatures significantly shortens the dissolution times of MnO_2 for the reducing agent studied ($Fe_{(res)}$). This is consistent with the results obtained by Zakeri et al. [50] with the use of ferrous ions and Bafghi et al. [51] for sponge iron. In the study carried out by Bafghi et al. [51], extractions close to 100% Mn were obtained, for times less than 5 min, a $Fe_{(res)}/MnO_2$ molar ratio of 2 and a sulfuric acid/MnO_2 molar ratio of 4. The results of the present study are quite similar to those obtained by Bafghi et al. [51], where a lower concentration of acid was used. When working at a temperature of 60 °C, the kinetics of Mn dissolution drastically increases, which agrees with the study carried out by Saldana et al. [48], where an analytical model was carried out to study various operational variables for the extraction of manganese from marine nodules in an acid medium, and tailings with a high content of Fe_3O_4 as a reducing agent. In their study, the researchers indicate that when working with Fe_3O_4/marine nodule ratios of 2/1 or higher and/or moderate temperatures (50 °C), the rest of the operational variables become irrelevant, and Mn extractions can be obtained over 60% in time periods pf less than 5 min.

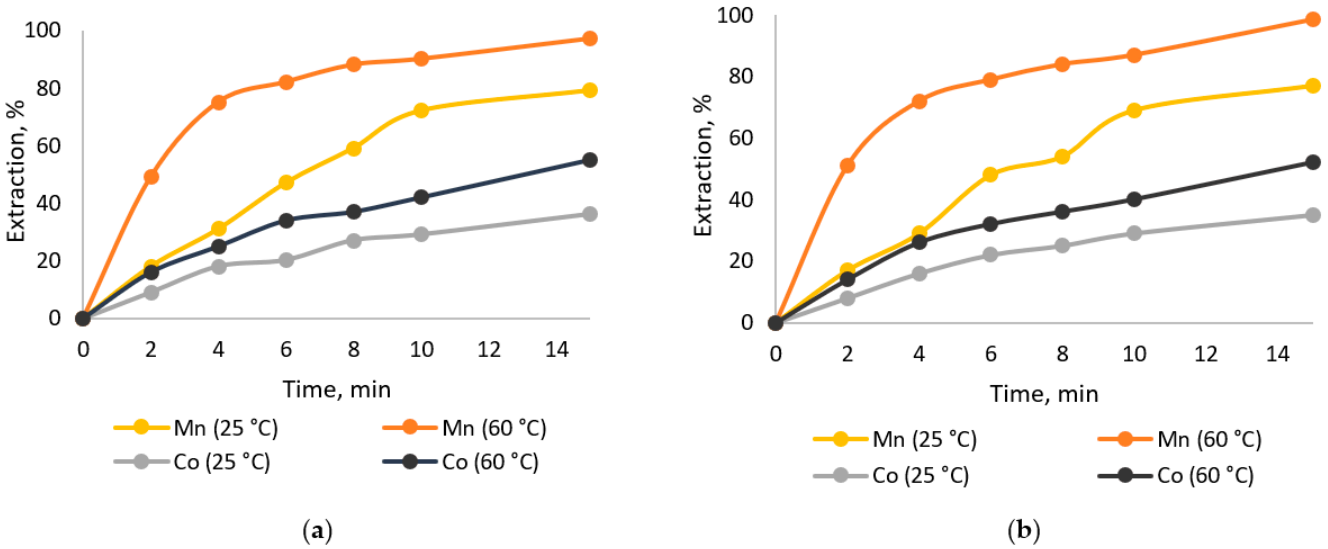

Figure 11. Effect of temperature on the dissolution of Mn and Co from marine nodules, marine nodule/$Fe_{(res)}$ ratio of 1/2, 600 rpm, −140 to +100 µm, H_2SO_4 concentration of 0.1 mol/L. (**a**) Sample 1, (**b**) Sample 2.

On the other hand, for cobalt extractions from marine nodules, the same tendency can be observed as when extracting manganese in an acid-reducing medium, where, when working at higher concentrations of reducing agent and/or temperature, cobalt extraction increases. This agrees with other previous studies, such as the one carried out by Gosh et al. [36], where for the extraction of Cu, Mn, Ni and Co from marine nodules, work was carried out in an acid medium and using paper as a reducing agent. In their results, the researchers conclude that the optimal working conditions were at a sulfuric acid concentration of 7.56% (*v*/*v*), time 2 h, paper 6 g/20 g marine nodule and temperature of 90 °C, achieving recoveries of 99% Mn and 97.9% Co. Additionally, in the study carried out by Hariprasad et al. [27] for the lixiviation of marine nodules in a reducing acid medium, the researchers indicate that the optimal working parameters were: sawdust 0.5 g/g of nodule, sulfuric acid 5% (*v*/*v*), temperature 105 °C and time 2 h, achieving extractions of 99.5% Mn and 93% Co.

Regarding the redox potential and pH values, in Figure 12 it can be seen that for the tests carried out, the pH range was between −0.5 and 0.2 and potential was between −0.7 and 1.5 V. These values favor the acid-reducing dissolution of Mn mainly, although

during some periods it is outside the range to effectively dissolve Co (0.8 and −0.25 V), which explains the lower extractions of this element with respect to Mn. On the other hand, these ranges of potential and pH due to the high concentration of reducing agent in the system favor the regeneration of ferric and ferrous ions avoiding the precipitation of Mn and Co [34].

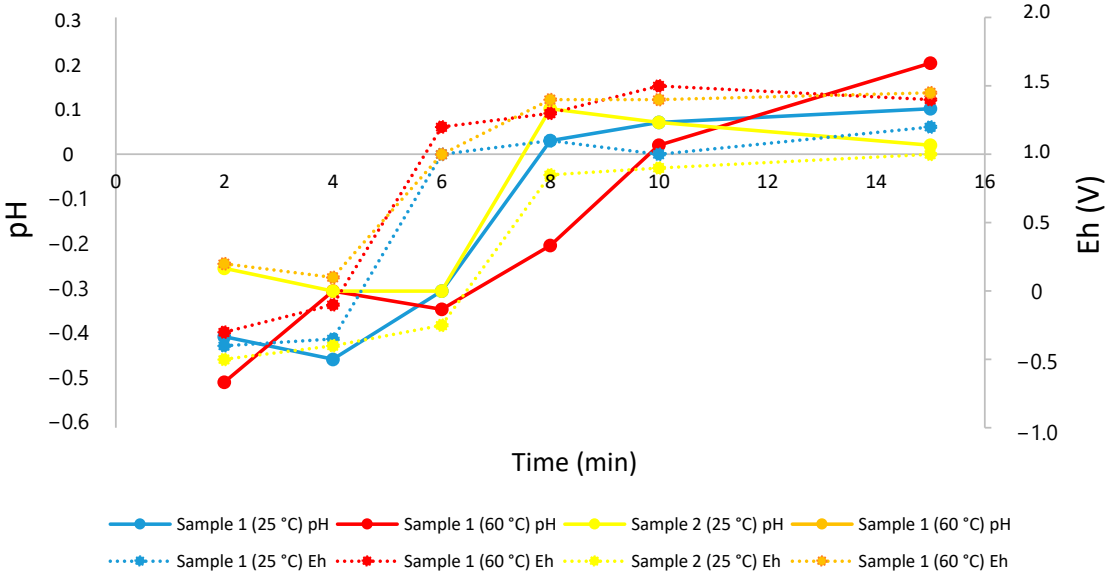

Figure 12. Effect of redox potential and pH on the extraction of Mn and Co (for the results of Figure 7).

3.3. Residue Analysis

In general, after the experiment for the two studied nodule samples (samples 1 and 2), neither the formation of contaminating elements nor the precipitation of manganese and cobalt compounds was observed. In previous studies [34,52], it has been mentioned that the presence of Fe^{2+} and Fe^{3+} ions allows maintaining the system potential ranging from 0.4 to 1.4 V and pH between 2 and 0.1 avoiding manganese precipitation.

3.3.1. Sample 1

Figure 13 shows a detailed view of a waste surface, which consists mainly of particles with Fe/S/O, Si/S/O, Ca/Mg/Si/O, Ca/O, Ca/S/O, Ca/S/O, Al/Si/O, Fe/O, Ca/Si/O, Ca/Ti/O, Ti/Si/O and Fe/Mn/Ti/S/O associations.

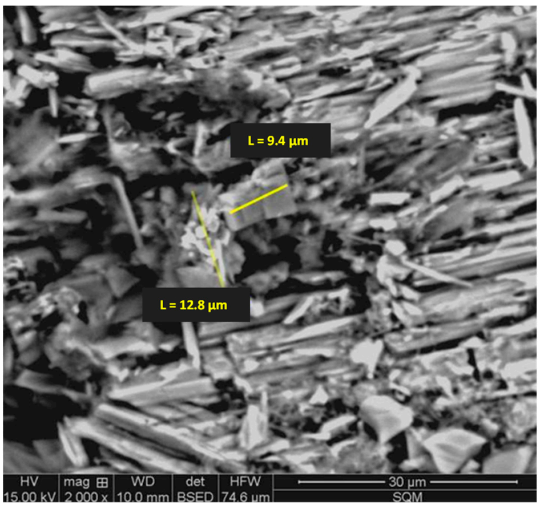

Figure 13. Scanning electron microscopy (SEM-EDS) micrograph of residue of sample 1. Magnification 2000×.

In Figure 14, the residual associations are detailed with colors:

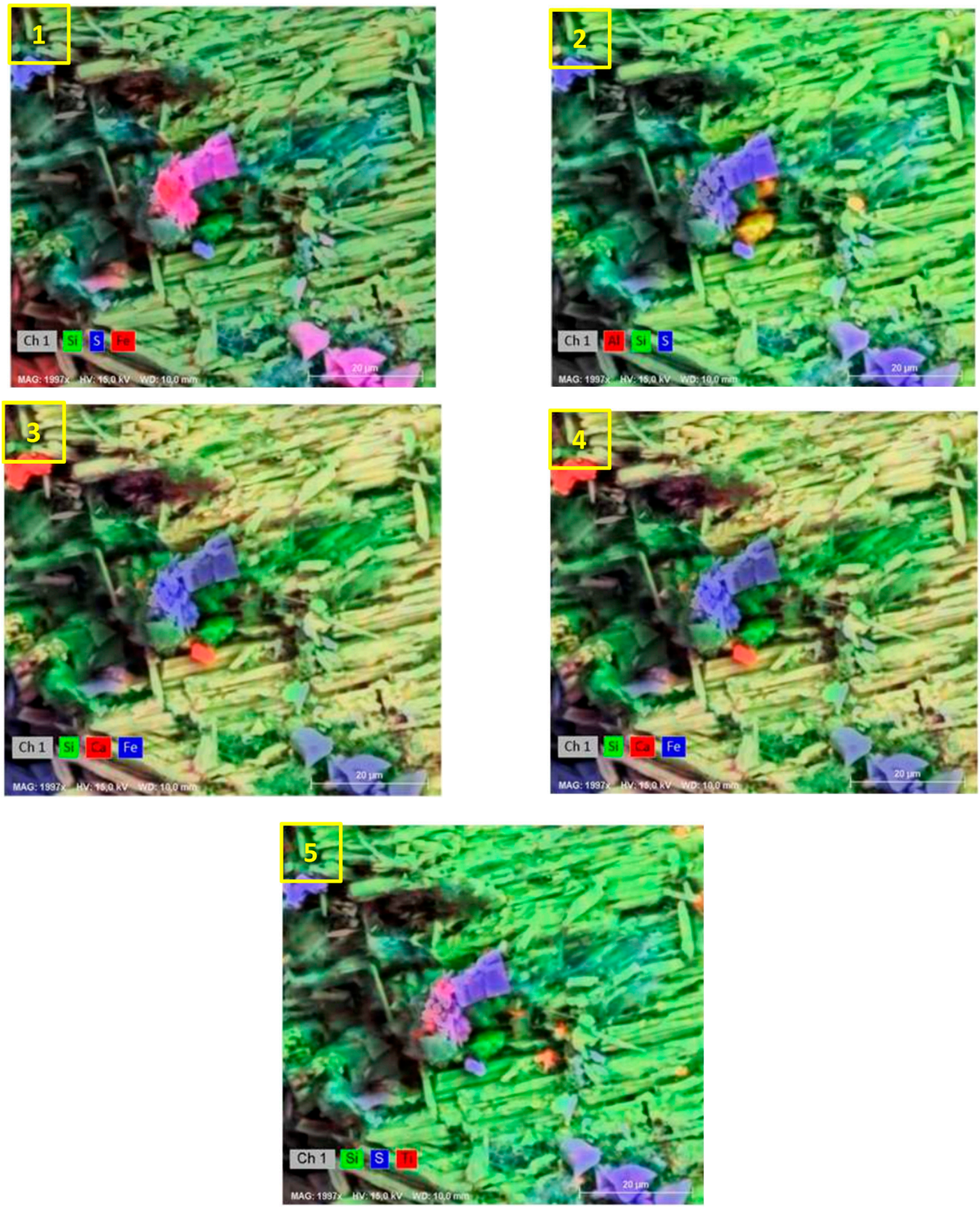

Figure 14. SEM micrograph with EDS analysis (color change) of residue sample 1. 2000× magnification.

Ca/Mg/Si/O (green coloration in (1) and (2), yellow in (3) and (4) and green in (5)), Fe/S/O (pink coloration in (1) and blue in (2), (3), (4) and (5)), Si/S/O (light blue coloration in (1) and (2), green in (3) and (4) and light blue in (5)), Al/Si/O (green coloration in (1), yellow in (2) and green in (3), (4) and (5)), Ca/S/O (blue coloration in (1) and (2), colorless

in (3), red in (4) and blue in (5)), Ti/Si/O (green coloration in (1), (2), (3) and (4) and yellow in (5)) and Fe/Mn/Ti/S/O (pink coloration in (1), blue in (2), (3) and (4) and pink in (5)).

Fort the Sample 1 neither the formation of contaminating elements nor the precipitation of manganese and cobalt compounds was observed (see Figure 15)

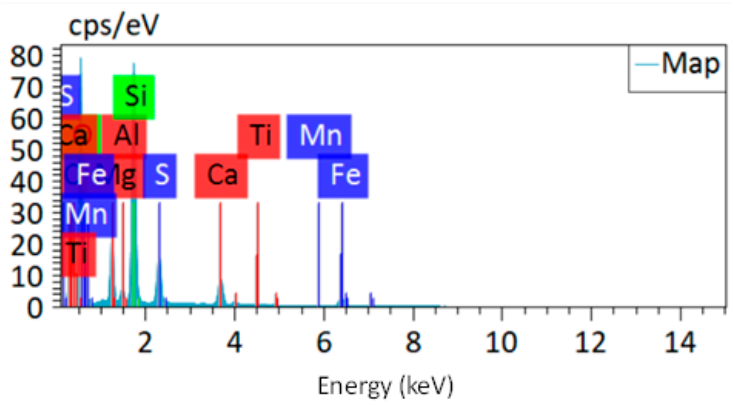

Map

Element	Mass Norm. (%)	Atom (%)	Abs. Error (%) (1 sigma)
O	44.52	48.09	5.06
C	23.98	34.51	2.82
Si	14.55	8.95	0.69
Ca	4.16	1.79	0.16
Fe	4.03	1.25	0.15
Mg	3.92	2.79	0.25
S	3.75	2.02	0.17
Al	0.78	0.50	0.06
Ti	0.20	0.07	0.03
Mn	0.11	0.04	0.03
	100	100	

Figure 15. Scanning electron microscopy elemental analysis for sample residue 1 (SEM-EDS).

3.3.2. Sample 2

Figure 16 shows a detailed view of the surface of a particle formed mainly by Fe/S/O and Si/S/O associations with Fe/O, Ca/Mg/Fe/Si/O, Al/Si/O and Ca/S/O impurities. Two types of particles with sulfate associations were observed, the first being Fe/S/O with a size range from 7.6 µm to 30.1 µm in length, and the second being Si/S/O with a size ranging from 29.0 to 215.9 µm in length.

Figure 16. Micrograph of residue of sample 2 obtained with scanning electron microscopy (SEM-EDS). Magnification 2000×.

In Figure 17, the residue associations are detailed with colors:

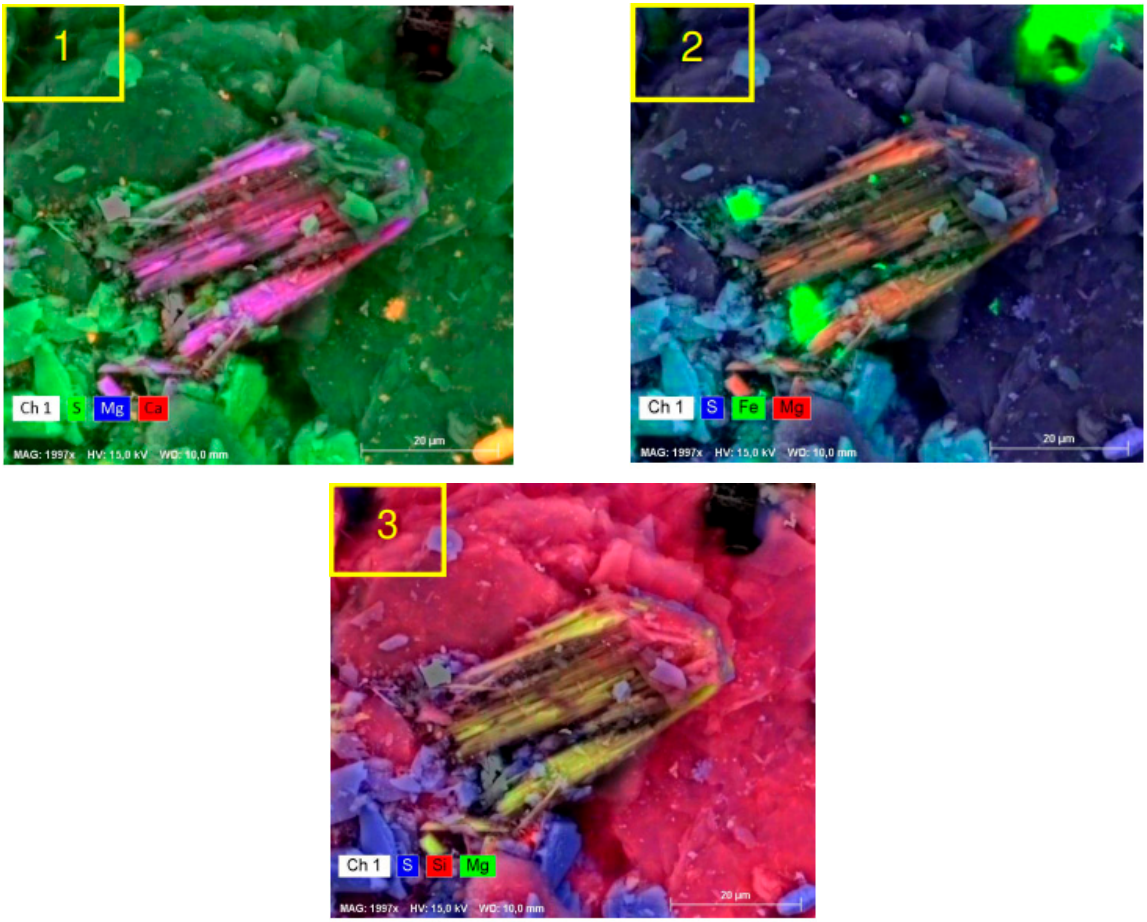

Figure 17. SEM micrograph with EDS analysis (color change) of residue sample 2, 2000× magnification.

Ca/Mg/Fe/Si/O (pink coloration in (1), orange in (2) and yellow in (3) of 46.3 µm in length, which is attached to particles of Si/S/O (dark green coloration in (1), dark blue in (2) and fuchsia in (3)) and Fe/S/O (green coloration in (1), cyan in (2) and blue in (3)), in addition to impurities of Ca/S/O (orange coloration in (1), blue in (2) and (3)) and Fe/O (no coloration in (1), green in (2) and no coloration in (3)). Al is detected in the spectrum, but its associations are not detected.

Fort the Sample 2 neither the formation of contaminating elements nor the precipitation of manganese and cobalt compounds was observed (see Figure 18)

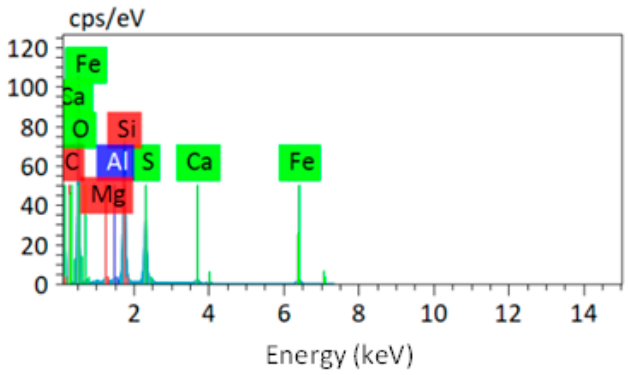

Map

Element	Mass Norm. (%)	Atom (%)	Abs. Error (%) (1 sigma)
O	54.24	60.61	5.06
Si	17.15	19.16	0.74
S	10.43	11.66	0.39
Fe	5.28	5.90	0.18
Ca	1.24	1.38	0.06
Mg	0.63	0.71	0.06
Al	0.52	0.58	0.05
	100	100	

Figure 18. Elemental analysis by scanning electron microscopy for sample residue 2 (SEM-EDS).

4. Conclusions

In the present study, the extraction of Co and Mn from two samples of marine nodules from different areas was investigated in an acid medium (0.1 mol/L of H_2SO_4), at medium temperature (25–60 °C), with the addition of an iron residue from the steel industry as a reducing agent (nodule/$Fe_{(res)}$ ratio of 1/2). The main findings are the following:

- Working with high concentrations of Fe in an acid-reducing medium allows maintaining the ranges of potential (0.8 and −0.25 V) and pH (−2 and 4.5) in the necessary values for the joint dissolution of Mn and Co.
- Increasing the system temperature significantly shortens the dissolution times of Mn and Co when working in an acid-reducing medium, adding iron residue.
- At room temperature (25 °C), in a time period of 15 min, extractions of ~80% of Mn and ~35% of Co are achieved, while working at 60 °C, in a time period of 15 min, the extractions for each element are ~98% Mn and ~55% Co.
- The formation of polluting elements was not observed, nor the precipitation of Mn and Co species in the studied residues.

In future works, it is necessary to study an economic mechanism to recover the manganese present in the solution. Zero-valent iron can be a good alternative, reusing waste from the metal finishing industry. This will allow a simple and low-cost process to recover manganese and cobalt from marine nodules.

Author Contributions: K.P. and N.T. contributed in investigation and wrote paper. P.R., F.J.G. and E.M. contributed with resources. S.G., E.G. and P.C.H. contributed with supervision and validation. All authors have read and agreed to the published version of the manuscript.

Funding: This research was funded by project Fondecyt 1221702 and European project GSEU (HORIZON-CL5-2021-D3-02-14, Project101075609).

Data Availability Statement: The data presented in this study are available on request from the corresponding author. The data are not publicly available due to chemical analysis laboratory restrictions.

Acknowledgments: Pedro Robles thanks project Fondecyt 1221702 for supporting this investigation and the Pontificia Universidad Catolica de Valparaiso for the support provided. Kevin Perez acknowledges the infrastructure and support of the PhD Program in Mineral Processes Engineering of the Universidad de Antofagasta. This research was partially funded by the European project GSEU (HORIZON-CL5-2021-D3-02-14, Project101075609). The authors thank all the scientific and technical staff who participated in the oceanographic cruises of the TASYO project onboard the R/V Cornide de Saavedra for data acquisition and for their expertise in collecting the samples.

Conflicts of Interest: The authors declare no conflict of interest.

References

1. Glasby, G.P.; Li, J.; Sun, Z. Deep-Sea Nodules and Co-rich Mn Crusts. *Mar. Georesour. Geotechnol.* **2015**, *33*, 72–78. [CrossRef]
2. Murray, J.; Irvine, R. XXXII.—On the Manganese Oxides and Manganese Nodules in Marine Deposits. *Trans. R. Soc. Edinb.* **1895**, *37*, 721–742. [CrossRef]
3. Ochromowicz, K.; Aasly, K.; Kowalczuk, P. Recent Advancements in Metallurgical Processing of Marine Minerals. *Minerals* **2021**, *11*, 1437. [CrossRef]
4. Sparenberg, O. A historical perspective on deep-sea mining for manganese nodules, 1965–2019. *Extr. Ind. Soc.* **2019**, *6*, 842–854. [CrossRef]
5. Toro, N.; Gálvez, E.; Saldaña, M.; Jeldres, R.I. Submarine mineral resources: A potential solution to political conflicts and global warming. *Miner. Eng.* **2022**, *179*, 107441. [CrossRef]
6. González, F.J.; Medialdea, T.; Schiellerup, H.; Zananiri, I.; Ferreira, P.; Somoza, L.; Monteys, X.; Alcorn, T.; Marino, E.; Lobato, A.B.; et al. MINDeSEA: Exploring seabed mineral deposits in European seas, metallogeny and geological potential for strategic and critical raw materials. *Geol. Soc. Lond. Spec. Publ.* **2023**, *526*. [CrossRef]
7. Hein, J.R.; Koschinsky, A.; Kuhn, T. Deep-ocean polymetallic nodules as a resource for critical materials. *Nat. Rev. Earth Environ.* **2020**, *1*, 158–169. [CrossRef]
8. Kang, J.; Wang, Y.; Qiu, Y. The effect of Fe^{3+} ions on the electrochemical behaviour of ocean manganese nodule reduction leaching in sulphuric acid solution. *RSC Adv.* **2022**, *12*, 1121–1129. [CrossRef]

9. Bau, M.; Schmidt, K.; Koschinsky, A.; Hein, J.; Kuhn, T.; Usui, A. Discriminating between different genetic types of marine ferro-manganese crusts and nodules based on rare earth elements and yttrium. *Chem. Geol.* **2014**, *381*, 1–9. [CrossRef]
10. Corathers, L.A. Manganese Statistics and Information. Available online: https://www.usgs.gov/centers/nmic/manganese-statistics-and-information (accessed on 1 March 2023).
11. Torres Albornoz, D.A. *Copper and Manganese Extraction through Leaching Processes*; Universidad Politécnica de Cartagena: Cartagena, Spain, 2021.
12. Banza Lubaba Nkulu, C.; Casas, L.; Haufroid, V.; De Putter, T.; Saenen, N.D.; Kayembe-Kitenge, T.; Musa Obadia, P.; Kyanika Wa Mukoma, D.; Lunda Ilunga, J.M.; Nawrot, T.S.; et al. Sustainability of artisanal mining of cobalt in DR Congo. *Nat. Sustain.* **2018**, *1*, 495–504. [CrossRef]
13. Hein, J.R.; Mizell, K.; Koschinsky, A.; Conrad, T.A. Deep-ocean mineral deposits as a source of critical metals for high- and green-technology applications: Comparison with land-based resources. *Ore Geol. Rev.* **2013**, *51*, 1–14. [CrossRef]
14. Kuhn, T.; Rühlemann, C. Exploration of Polymetallic Nodules and Resource Assessment: A Case Study from the German Contract Area in the Clarion-Clipperton Zone of the Tropical Northeast Pacific. *Minerals* **2021**, *11*, 618. [CrossRef]
15. Toro, N.; Robles, P.; Jeldres, R.I. Seabed mineral resources, an alternative for the future of renewable energy: A critical review. *Ore Geol. Rev.* **2020**, *126*, 103699. [CrossRef]
16. Cifuentes, C. *Chile, Minería Más Allá del Cobre*; Cochilco: Santiago, Chile, 2019.
17. Hoover, M.; Han, K.N.; Fuerstenau, D.W. Segregation roasting of nickel, copper and cobalt from deep-sea manganese nodules. *Int. J. Miner. Process* **1975**, *2*, 173–185. [CrossRef]
18. Sommerfeld, M.; Friedmann, D.; Kuhn, T.; Friedrich, B. "Zero-Waste": A Sustainable Approach on Pyrometallurgical Processing of Manganese Nodule Slags. *Minerals* **2018**, *8*, 544. [CrossRef]
19. Su, K.; Ma, X.; Parianos, J.; Zhao, B. Thermodynamic and Experimental Study on Efficient Extraction of Valuable Metals from Polymetallic Nodules. *Minerals* **2020**, *10*, 360. [CrossRef]
20. Thoumsin, F.J.; Coussement, R. Fluid-bed roasting reactions of copper and cobalt sulfide concentrates. *JOM* **1964**, *16*, 831–834. [CrossRef]
21. Kawahara, M.; Tokikawa, K.; Mitsuo, T. Sulfating Roasting of Manganese Leaching of Roasted. *Shigen-Sozai* **1991**, *107*, 305–309. [CrossRef]
22. Pahlman, J.E.; Khalafalla, S.E. Selective Recovery of Nickel, Cobalt, Manganese from Sea Nodules with Sulfurous Acid. U.S. Patent Application No. 4,138,465; 860,249; 771,213, 6 February 1979.
23. Jana, R.K.; Akerkar, D.D. Studies of the Metal-Ammonia-Carbon Dioxide-Water System in Extraction Metallurgy of Polymetallic Sea Nodules. *Hydrometallurgy* **1989**, *22*, 363–378. [CrossRef]
24. Deng, X.; He, D.; Chi, R.; Xiao, C.; Hu, J. The Reduction Behavior of Ocean Manganese Nodules by Pyrolysis Technology Using Sawdust as the Reductant. *Minerals* **2020**, *10*, 850. [CrossRef]
25. Anand, S.; Das, S.C.; Das, R.P.; Jena, P.K. Leaching of manganese nodules at elevated temperature and pressure in the presence of oxygen. *Hydrometallurgy* **1988**, *20*, 155–167. [CrossRef]
26. Han, K.N.; Fuerstenau, D.W. Acid leaching of ocean manganese nodules at elevated temperatures. *Int. J. Miner. Process.* **1975**, *2*, 163–171. [CrossRef]
27. Hariprasad, D.; Mohapatra, M.; Anand, S. Reductive Leaching of Manganese Nodule Using Saw Dust in Sulphuric Acid Medium. *Trans. Indian Inst. Met.* **2018**, *71*, 2971–2983. [CrossRef]
28. Nayl, A.A.; Ismail, I.M.; Aly, H.F. Recovery of pure $MnSO_4 \cdot H_2O$ by reductive leaching of manganese from pyrolusite ore by sulfuric acid and hydrogen peroxide. *Int. J. Miner. Process.* **2011**, *100*, 116–123. [CrossRef]
29. Sinha, M.K.; Purcell, W. Reducing agents in the leaching of manganese ores: A comprehensive review. *Hydrometallurgy* **2019**, *187*, 168–186. [CrossRef]
30. Ehrlich, H.L. Manganese oxide reduction as a form of anaerobic respiration. *Geomicrobiol. J.* **1987**, *5*, 423–431. [CrossRef]
31. Dwivedi, D.; Randhawa, N.S.; Saroj, S.; Jana, R.K. An Overview of Manganese Recovery by Hydro and Pyro-Metallurgical Routes. *J. Inst. Eng. Ser. D* **2017**, *98*, 147–154. [CrossRef]
32. Kowalczuk, P.B.; Manaig, D.O.; Drivenes, K.; Snook, B.; Aasly, K.; Kleiv, R.A. Galvanic leaching of seafloor massive sulphides using MnO_2 in H_2SO_4-NaCl media. *Minerals* **2018**, *8*, 235. [CrossRef]
33. Naik, P.K.; Sukla, L.B.; Das, S.C. Aqueous SO_2 leaching studies on Nishikhal manganese ore through factorial experiment. *Hydrometallurgy* **2000**, *54*, 217–228. [CrossRef]
34. Toro, N.; Rodríguez, F.; Rojas, A.; Robles, P.; Ghorbani, Y. Leaching manganese nodules with iron-reducing agents—A critical review. *Miner. Eng.* **2021**, *163*, 106748. [CrossRef]
35. Acharya, R.; Ghosh, M.; Anand, S.; Das, R. Leaching of metals from Indian ocean nodules in SO_2–H_2O–H_2SO_4–$(NH_4)_2SO_4$ medium. *Hydrometallurgy* **1999**, *53*, 169–175. [CrossRef]
36. Ghosh, M.K.; Barik, S.P.; Anand, S. Sulphuric acid leaching of polymetallic nodules using paper as a reductant. *Trans. Indian Inst. Met.* **2008**, *61*, 477–481. [CrossRef]
37. Mishra, D.; Srivastava, R.R.; Sahu, K.K.; Singh, T.B.; Jana, R.K. Leaching of roast-reduced manganese nodules in NH_3–$(NH_4)_2CO_3$ medium. *Hydrometallurgy* **2011**, *109*, 215–220. [CrossRef]
38. Torres, D.; Ayala, L.; Saldaña, M.; Cánovas, M.; Nieto, S.; Castillo, J.; Robles, P.; Toro, N. Leaching manganese nodules in an acid medium and room temperature comparing the use of different fe reducing agents. *Metals* **2019**, *9*, 1316. [CrossRef]

39. Martin, S. Precipitation and Dissolution of Iron and Manganese Oxides. In *Environmental Catalysis*; CRC Press: Boca Raton, FL, USA, 2005; pp. 61–82.
40. Toro, N.; Jeldres, R.I.; Órdenes, J.A.; Robles, P.; Navarra, A. Manganese Nodules in Chile, an Alternative for the Production of Co and Mn in the Future—A Review. *Minerals* **2020**, *10*, 674. [CrossRef]
41. Bezerra, M.A.; Santelli, R.E.; Oliveira, E.P.; Villar, L.S.; Escaleira, L.A. Response surface methodology (RSM) as a tool for optimization in analytical chemistry. *Talanta* **2008**, *76*, 965–977. [CrossRef]
42. David, H.A.; Edwards, A.W.F. *Annotated Readings in the History of Statistics*; Springer Series in Statistics; Springer: New York, NY, USA, 2009; ISBN 978-0-387-98134-5.
43. Bettonvil, B.; del Castillo, E.; Kleijnen, J.P.C. Statistical testing of optimality conditions in multiresponse simulation-based optimization. *Eur. J. Oper. Res.* **2009**, *199*, 448–458. [CrossRef]
44. Cintas, P.G.; Almagro, L.M.; Llabres, X.T.-M. *Industrial Statistics with Minitab*; Wiley: Hoboken, NJ, USA, 2012; ISBN 978-0470972755.
45. Minitab LLC. *Getting Started with Minitab 18*; Minitab Inc.: State College, PA, USA, 2017; Volume 73.
46. Montgomery, D.C.; Runger, G.C. *Applied Statistics and Probalisty for Engineers*; John Wiley & Sons: Hoboken, NJ, USA, 2014; ISBN 9781118539712.
47. Devore, J. *Probability & Statistics for Engineering and the Sciences*, 8th ed.; Butterworth-Heinemann: Oxford, UK, 2010; ISBN 0-538-73352-7.
48. Saldaña, M.; Toro, N.; Castillo, J.; Hernández, P.; Trigueros, E.; Navarra, A. Development of an analytical model for the extraction of manganese from marine nodules. *Metals* **2019**, *9*, 903. [CrossRef]
49. Senanayake, G. Acid leaching of metals from deep-sea manganese nodules—A critical review of fundamentals and applications. *Miner. Eng.* **2011**, *24*, 1379–1396. [CrossRef]
50. Zakeri, A. Dissolution Kinetics of Manganese Dioxide Ore in Sulfuric Acid in the Presence of Ferrous Ion. *Iran. J. Mater. Sci. Eng.* **2007**, *4*, 22–27.
51. Bafghi, M.S.; Zakeri, A.; Ghasemi, Z.; Adeli, M. Reductive dissolution of manganese ore in sulfuric acid in the presence of iron metal. *Hydrometallurgy* **2008**, *90*, 207–212. [CrossRef]
52. Moraga, C.; Cerecedo-Saenz, E.; González, J.; Robles, P.; Carrillo-Pedroza, F.R.; Toro, N. Comparative Study of MnO_2 Dissolution from Black Copper Minerals and Manganese Nodules in an Acid Medium. *Metals* **2021**, *11*, 817. [CrossRef]